Planetary Wave Breaking and Nonlinear Reflection: Seasonal Cycle and Interannual Variability

JOHN T. ABATZOGLOU AND GUDRUN MAGNUSDOTTIR

Department of Earth System Science, University of California, Irvine, Irvine, California

(Manuscript received 7 July 2005, in final form 24 April 2006)

ABSTRACT

Forty-six years of daily averaged NCEP–NCAR reanalysis data are used to identify the occurrence of planetary wave breaking (PWB) in the subtropical upper troposphere. As large-amplitude waves propagate into the subtropics where the zonal flow is weak, they may break. PWB is diagnosed by observing the large-scale meridional overturning of potential vorticity (PV) contours on isentropic surfaces near the subtropical tropopause. PWB occurs most often during summer, and almost exclusively over the subtropical ocean basins in the Northern Hemisphere. The seasonal evolution of the zonal flow (and the associated latitudinal PV gradient) regulates the location and frequency of PWB. Significant interannual variability in PWB is associated with well-known modes of climate variability.

One of the most interesting dynamical consequences of PWB is the possibility of nonlinear reflection poleward out of the wave-breaking region. Modeling studies have found nonlinear reflection following PWB. Observations show that about 36% of all PWB events are followed by nonlinear reflection back into midlatitudes. In these cases, a poleward-arching wave train can be seen propagating away from the wave-breaking region following breaking. It is suggested that a sufficiently strong latitudinal PV gradient must be present downstream of the wave-breaking region for reflection to take place. The proportion of PWB events that is reflective stays rather constant through the year, with slightly higher numbers in spring and fall compared to those in winter and summer.

1. Introduction

The quasi-stationary planetary waves of the extratropics exist on a westerly background flow (Held et al. 2002). As wave trains propagate to lower latitudes they encounter weaker zonal flow. Small-amplitude wave trains may be "absorbed" as they approach the critical latitude—that at which the phase speed of the waves matches the background flow field. This means that the wave train weakens and disappears (resulting from radiative damping) without mixing up the potential vorticity (PV) field and affecting the large-scale flow. If the wave amplitude is large enough, waves may break and mix up PV over a finite region. Planetary wave breaking (PWB) is manifested by the large-scale and rapid, irreversible overturning of PV contours on isentropic surfaces (McIntyre and Palmer 1983). The ability of planetary waves to irreversibly stir up the PV field depends not only on wave amplitude but also on the strength of the latitudinal PV gradient. The stronger the PV gradient, the greater the ability of the PV field to support linear wave propagation and resist wave breaking.

Examples of PWB are shown in Fig. 1. The quasi-horizontal PV field on the 350-K isentropic surface is shown on three consecutive days from 18 to 20 July 1997. Two separate PWB events in different stages of development are seen over the Pacific. The first event is observed near the date line on 19 July 1997. Note the large-scale anticyclonic advection of low (high) PV poleward (equatorward). A second event is noted near Japan on 20 July 1997. PWB events tend to cluster in time and space, thereby forming a "surf zone," which is a nomenclature used to describe the region surrounding the stratospheric polar vortex (McIntyre and Palmer 1983).

Planetary wave breaking can impact the large-scale atmospheric circulation both in the extratropics and the Tropics. In particular, the presence or absence of nonlinear reflection (or reradiation) out of the wave-breaking region can profoundly impact the extratropi-

Corresponding author address: Gudrun Magnusdottir, Department of Earth System Science, University of California, Irvine, Irvine, CA 92697-3100.
E-mail: gudrun@uci.edu

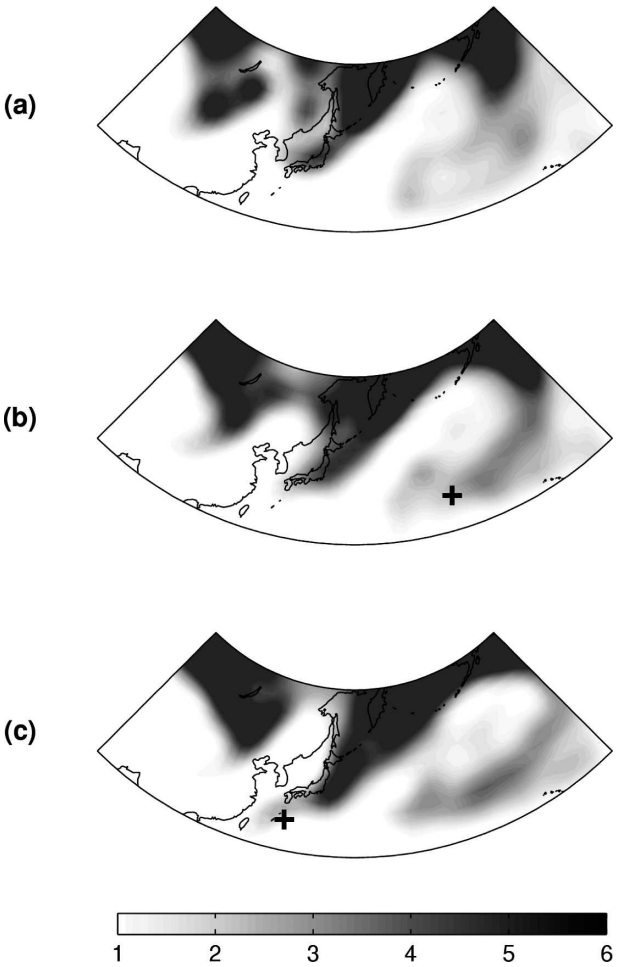

FIG. 1. PV (PVU) on the 350-K isentropic surface for a PWB event occurring on 19 Jul 1997. Daily averaged fields are shown from (a)–(c) one day prior to one day following the event. The spot where breaking is detected is indicated by a plus sign (+).

cal flow field (Abatzoglou and Magnusdottir 2006). We have recently found evidence of nonlinear reflection of tropospheric planetary waves in 44 yr of reanalysis data (Abatzoglou and Magnusdottir 2004). Our study employed an objective algorithm to first identify PWB events and then classify them as either reflective or nonreflective. This confirmed our expectation, based on a hierarchy of modeling studies, that PWB in the subtropics may result in the nonlinear reflection of planetary waves into midlatitudes (Brunet and Haynes 1996; Magnusdottir and Haynes 1999; Magnusdottir and Walker 2000; Walker and Magnusdottir 2002, 2003). Wave breaking is episodic and, furthermore, one would not expect all PWB events to result in nonlinear reflection. Nonconservative effects are important in the real atmosphere. These effects can lead to the absorption of wave activity within the wave-breaking region, thus inhibiting nonlinear reflection.

Impacts of PWB on tropical dynamics have been demonstrated, for example, by Kiladis (1998), who showed how the influx of PV-rich air into the Tropics can lead to convective outbreaks. PWB may also lead to stratosphere–troposphere exchange along quasi-horizontal isentropes between the extratropical lower stratosphere (high PV) and the upper troposphere (low PV) of the subtropics/Tropics. This large-scale interaction can modify temperature and static stability, as well as water vapor and ozone concentration of the upper troposphere and lower stratosphere (Holton et al. 1995).

This paper examines the frequency of occurrence of PWB and nonlinear reflection using 46 yr of reanalysis data. We examine the spatial and temporal distribution of PWB events as they relate to the seasonal evolution of the zonal flow as well as interannual variability associated with the major climate modes. The plan of the paper is as follows. In section 2, we describe the datasets and analysis methods used to identify PWB and nonlinear reflection. Section 3 provides an overview of the distribution of PWB both in space and through the annual cycle. Interannual variability is analyzed in section 4, with emphasis on variability associated with the East Asian summer monsoon (EASM), El Niño–Southern Oscillation (ENSO), and the North Atlantic Oscillation (NAO). In section 5, we discuss nonlinear reflection and what role the latitudinal PV gradient appears to play in determining whether reflection may take place following PWB. Section 6 contains some concluding remarks.

2. Data and analysis

We use 46 yr (1958–2003) of daily averaged fields of temperature, geopotential, and velocity from NCEP–NCAR reanalysis data. The data are of 2.5° horizontal resolution, on the 100-, 150-, 200-, 250-, 300-, 400-, and 500-hPa pressure levels. While this dataset may not capture finer-scale features of Rossby wave breaking, the resolution is sufficient for diagnosing the large-scale wave-breaking events (PWB) that we wish to identify. We proceed to calculate PV on isentropic surfaces by first interpolating the velocity field to isentropic surfaces using log-linear interpolation, and applying second-order centered finite differencing for horizontal derivatives. Vertical derivatives are computed using cubic-spline interpolation.

Accounting for variations in the subtropical tropopause involves analyzing PV on several isentropic surfaces that may intersect it. We chose to identify PWB on the following four isentropic surfaces in the upper troposphere/lower stratosphere: 330, 340, 350, and

360 K. In previous studies (i.e., Postel and Hitchman 1999; Abatzoglou and Magnusdottir 2004), PWB was diagnosed by examining PV on the 350-K surface only. Although the 350-K surface best approximates the average level of the subtropical tropopause in summer, including the additional three isentropic surfaces is crucial for detecting a wider range of subtropical breaking events in different seasons.

Figure 2 shows the seasonal mean latitudinal profile of potential temperature on the 2-PVU (potential vorticity unit = 10^{-6} K m^2 s^{-1} kg^{-1}) surface over the Atlantic and Pacific basins during winter [December–February (DJF)], spring [March–May (MAM)], summer [June–August (JJA)], and fall [September–November (SON)], respectively, derived from 42 yr of 40-yr European Centre for Medium-Range Weather Forecast (ECMWF) Re-Analysis (ERA-40) monthly mean data. For each season and ocean basin, we averaged over a sector 30° in longitude centered around the longitude of the most frequent PWB. The signature of breaking, which is especially apparent in JJA (Fig. 2c), is manifested in a flat potential temperature profile over a latitudinal stretch of about 20°–35°N over the Pacific, and of about 28°–38°N over the Atlantic. Regions with almost constant potential temperature as a function of latitude on a constant PV surface are indicative of frequent PWB. Note that the subtropical tropopause is highest in summer and lowest in winter. We find that for all seasons the region of greatest PV mixing occurs slightly poleward and on a lower isentropic surface over the Atlantic than over the Pacific.

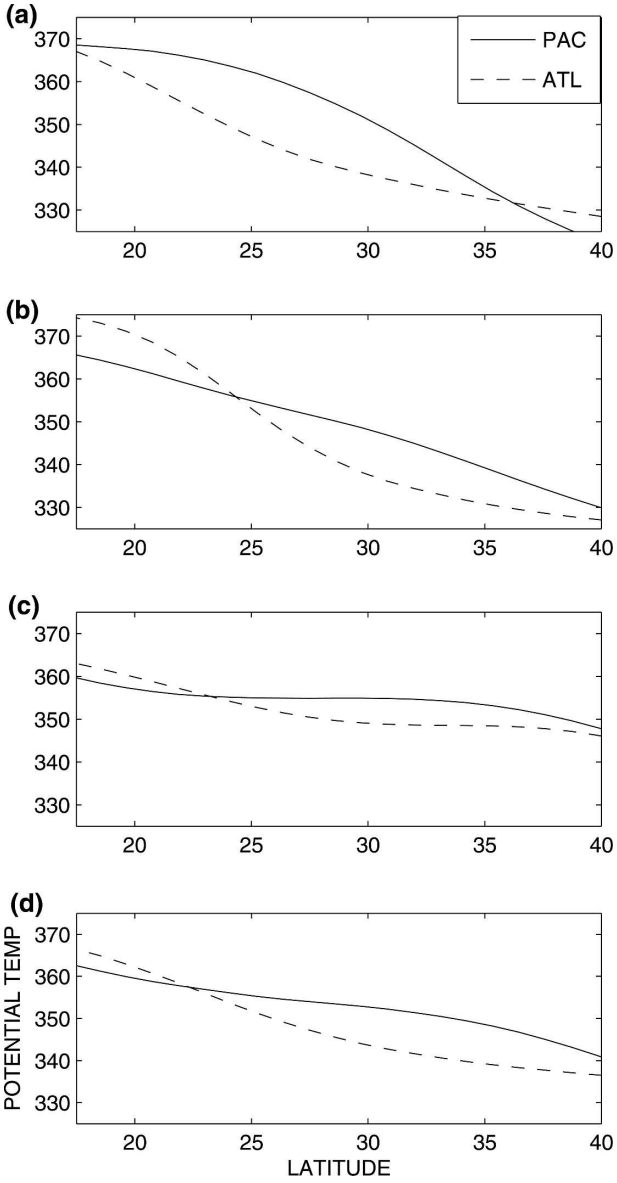

FIG. 2. Seasonal mean of potential temperature on the 2-PVU surface as a function of latitude, averaged over 30° longitudinal sectors centered around the greatest concentration of PWB in each ocean basin for each season (from ERA-40 monthly mean data): (a) DJF, (b) MAM, (c) JJA, and (d) SON. Pacific values are indicated by solid curves, Atlantic values are indicated by dashed curves.

a. Diagnosing PWB

Most PWB events are the result of anticyclonic wave breaking. These events tend to occur on the equatorward (anticyclonic shear) side of the jet. Idealized modeling studies (e.g., Brunet and Haynes 1996; Magnusdottir and Walker 2000) show that the PV field during anticyclonic breaking resembles that of the Kelvin's cat's-eyes pattern, whereby high (low) PV rolls up anticyclonically equatorward (poleward), causing the wave to break. To capture episodes of anticyclonic wave breaking, we look for signals in the PV field similar to those seen in the modeling studies. Although there is no single unique signature of wave breaking (McIntyre and Palmer 1983), we attempt to objectively identify PWB events equatorward of the subtropical jet, at 10°–40° latitude on each day and on each of the four isentropic surfaces. By constraining our analysis in latitude to areas equatorward of the jet, and in the vertical to isentropic surfaces that intersect the tropopause in the subtropics, we are avoiding baroclinic eddies that tend to break on lower isentropic surfaces farther poleward. PWB events are diagnosed if they satisfy the following criteria involving the large-scale PV field. In the Southern Hemisphere (SH) PV is negative. We therefore implement the absolute value of PV in the following algorithm.

1) There is a reversal in the latitudinal PV gradient about the tropopause such that a region of high PV

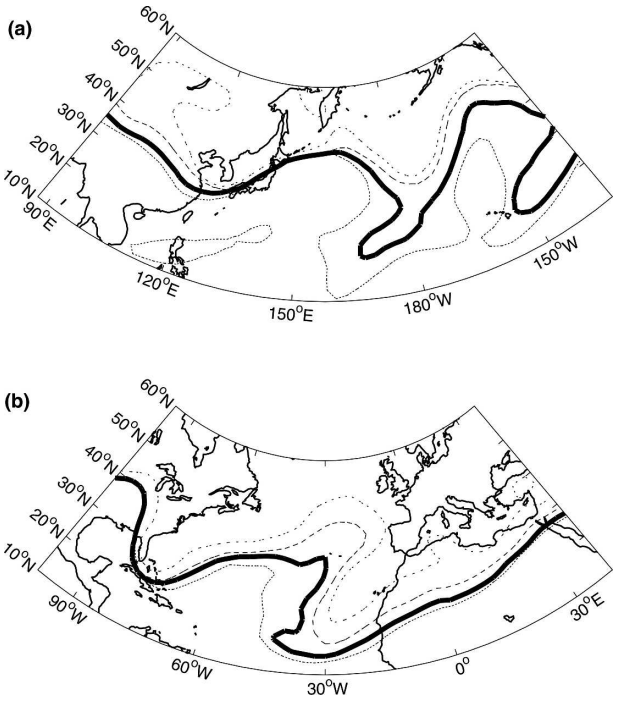

FIG. 3. The 2-PVU contour on the 360- (finely dotted), 350- (solid thick), 340- (dashed), and 330-K (dotted) surfaces for PWB events occurring on (a) 11 Jun 1997 (Pacific), and (b) 26 Dec 1994 (Atlantic).

(PV $\geq$ 3 PVU) exists equatorward of a region of low PV (PV $\leq$ 1 PVU).

2) There is a localized eastward PV gradient about the break, consistent with the notion of anticyclonic breaking.
3) The region of high (low) PV is part of a tongue of PV originating in the extratropics (Tropics).[1]

To ensure that only one PWB event is counted per episode, we identify a "breaking point" as the southwesternmost point first satisfying the above criteria (see Fig. lb). All other PV reversals occurring within 30° longitude or within 4 days following the initial diagnosis are discarded. In many instances, the signature of PWB can be observed on multiple adjacent isentropic surfaces on the same day. If PWB is simultaneously identified on more than one isentropic surface, including the 350-K surface, the event is only counted at 350 K. If a PWB event is detected on both the 340- and 330-K surface, only the event at 340 K is counted.

Figure 3 shows PWB events in summer over the North Pacific (Fig. 3a) and in winter over the North Atlantic (Fig. 3b). The 2-PVU PV contour is depicted on the four different isentropic surfaces that we analyze. The event over the Pacific exhibits the signature of breaking on the 350- and 360-K isentropes only. In contrast, the event over the Atlantic breaks on all four isentropes. Even though both events are classified as 350-K PWB events, they are quite different in vertical extent. The example shown in Fig. 3a is typical of summertime events in the Pacific where PWB is often only observed on the uppermost isentropic surfaces. The winter events, occurring predominantly over the North Atlantic basin, tend to be deeper in vertical extent.

b. Diagnosing nonlinear reflection

Upon cataloging cases of PWB, we employ the stationary wave activity flux of Plumb (1985)[2] to detect those cases that show evidence of nonlinear reflection. Prior to PWB there is a strong equatorward wave activity flux associated with the equatorward-propagating wave train. Nonlinear reflection leads to a reversal in the wave activity flux (i.e., a poleward-directed flux) in the days following breaking (Magnusdottir and Haynes 1999). For each case of PWB, we compute the wave activity flux at 250 hPa using flow fields that are averaged in time 1–4 days following breaking. We then examine the latitudinal component of the flux, averaging over the area 15°–60° east and 10°–20° poleward of the breaking point (at the approximate latitude of the jet where the wave activity flux is well defined). Our previous modeling studies have shown that the strongest signal of reflection is found in this sector. PWB events with a poleward-directed component of wave activity flux are designated as reflective cases. We also computed the vertically integrated wave activity flux (400–100 hPa) to verify that the signal at 250 hPa is robust. Upon evaluating this flux for each individual case of wave breaking we are able to distinguish between those events showing signs of nonlinear reflection, and those that do not.

Spatially and temporally shifted fields from individual events are then composited for cases of reflective and nonreflective PWB. This allows for the analysis of robust features of wave breaking and the ensuing reflective/absorptive behavior.

3. Spatial and temporal distribution of PWB in the annual cycle

A total of 2655 PWB events were identified in the Northern Hemisphere (NH) over the 46-yr period.

[1] In other words, tongues of PV are attached to the reservoir of origin as opposed to being cutoff features.

[2] By definition, the basic state for this wave activity is the zonally averaged flow.

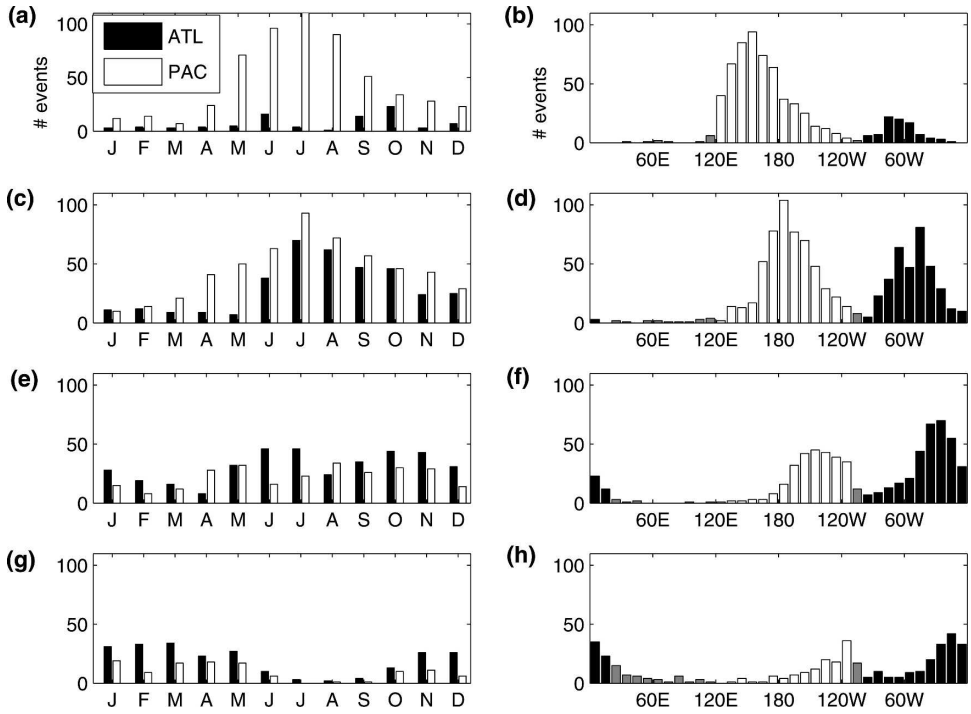

FIG. 4. Histograms of PWB in the NH on the (a), (b) 360-, (c), (d) 350-, (e), (f) 340-, and (g), (h) 330-K isentropic surfaces; PWB frequency is shown (left) by month and (right) by longitude. Events over the Atlantic are shown in black, events over the Pacific are shown in white. Events occurring at longitudes outside the two ocean basins are shown in gray.

Considerably fewer events, 134 over 46 yr, were identified in the SH. Because PWB is rare in the SH, we restrict the remainder of our discussion to PWB events in the NH.

The seasonality and longitudinal distribution of PWB on the four isentropic surfaces is shown in Fig. 4. Overall, 658, 924, 660, and 413 PWB events are detected on the 360-, 350-, 340-, and 330-K isentropic surfaces, respectively. Note that the algorithm for classifying the vertical location of breaking favors the 350-K surface if PWB is found to occur on any surface that includes 350 K (see section 2a). PWB is most prevalent between May and October (nearly 75% of all events); moreover, nearly all (95%) PWB events take place over the North Pacific and North Atlantic basins.

While PWB occurs more frequently over the Pacific (1510 events) than over the Atlantic (1048 events), other differences in PWB between the ocean basins are also apparent. The majority of PWB on the 360-K surface is observed over the Pacific in summer (Fig. 4a). The dramatic increase in PWB events on higher isentropic surfaces in summer results from the upward shifting of the tropopause over subtropical latitudes of Asia and the western Pacific in response to the onset of the Indian–Asian monsoonal circulation (e.g., Hsu et al. 2005; Hoinka 1999). Note the rarity of PWB over the Atlantic on the 360-K surface, even in summer where the regional maximum is instead found at 350 K. This finding is consistent with Fig. 2 as well as Fig. 3 of Hoinka (1999), suggesting that the subtropical tropopause over the Atlantic is lower in all seasons than that over the Pacific. Conversely, if we restrict the analysis to the 330-K surface, we observe nearly twice as many PWB events over the Atlantic than over the Pacific, with most occurring in winter. These findings highlight the importance of implementing PWB diagnostics on several isentropic surfaces.

Seasonal changes in the frequency and location of the wave-breaking regions correspond well with the strength and extent of the climatological jets as can be seen in Fig. 5. Regions of maximum breaking are located over the western ocean basins in summer, coincident with the westward contraction of the jets. Conversely, PWB occurs mainly over the eastern ocean basins in winter, coincident with the eastward extension of the jets. The wave-breaking regions are characterized by a weak latitudinal PV gradient located immediately downstream of a strong PV gradient where the upper-

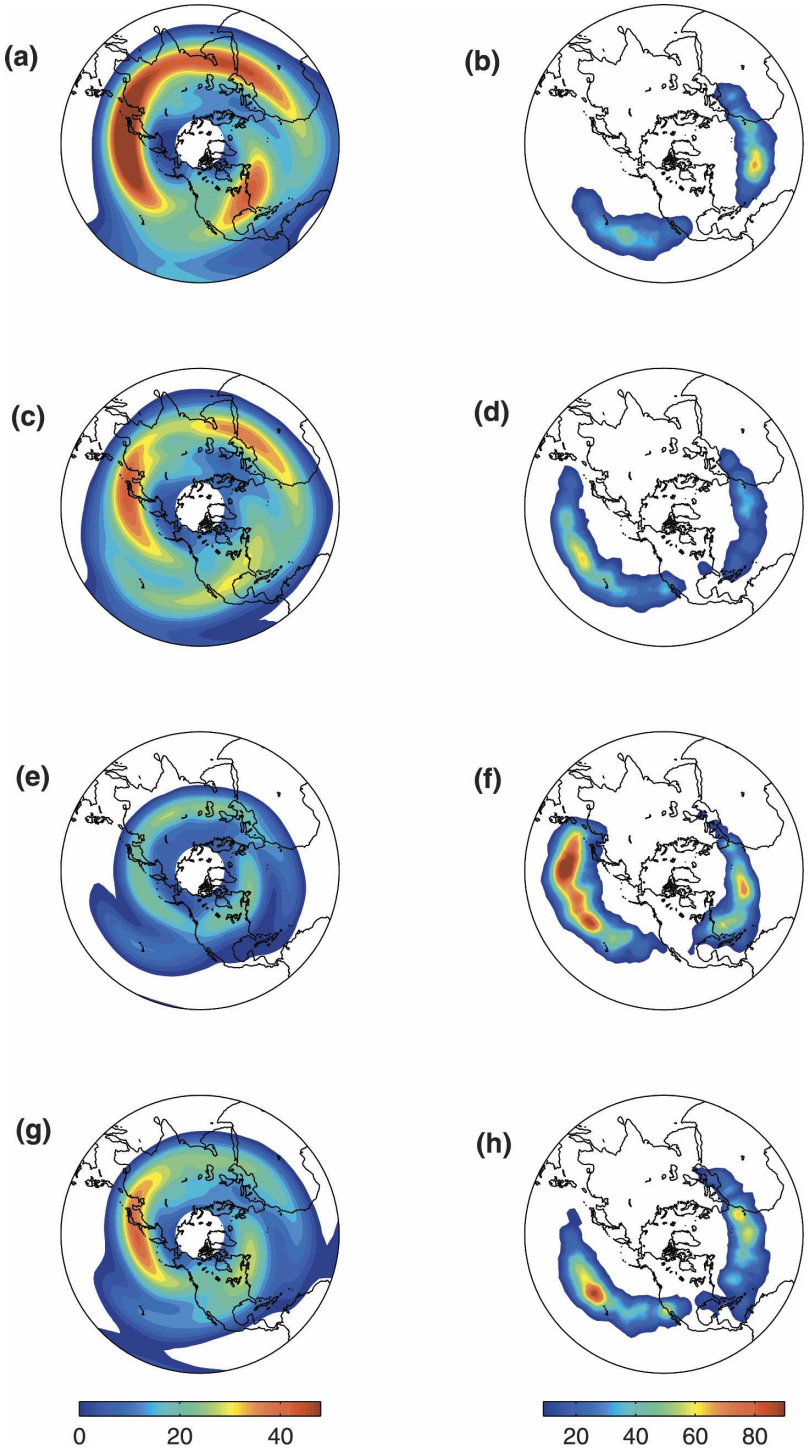

FIG. 5. (a) DJF, (c) MAM, (e) JJA, and (g) SON climatological 250-hPa zonal wind. Easterlies are shown in white; (b) DJF, (d) MAM, (f) JJA, and (h) SON number density of PWB events observed over the 46-yr period.

tropospheric flow is diffluent, near the jet exit regions. Wave breaking is observed to be episodic with prolonged periods of breaking. Our results show that a majority of PWB events occur close in space (within 50° longitude) and time (within 10 days) of a previous PWB event (see Fig. 1). The difference in the flow field between the two ocean basins goes hand in hand with differences in the distribution of PWB.

a. Pacific

In winter the Asian jet is located near 30°N with strong upper-tropospheric winds extending well into the central Pacific (Fig. 5a). The strong PV gradient (not shown) associated with the jet over the western Pacific provides ample support for the propagation of Rossby waves. As wave trains encounter the weaker PV gradient near the jet exit region, they acquire an equatorward component to their propagation, and as they approach the zero-wind line their amplitudes increase and they may break. Wave breaking takes place directly downstream and equatorward of the jet exit region near Hawaii where the flow is diffluent and the westerlies are weak (Fig. 5b). In winter, the PV gradient is usually strong over the entire basin, thus providing resistance to wave breaking (sometimes referred to as a PV barrier). Additionally, the zero-wind line is typically (but not always) located deep in the Tropics in winter. Consequently, PWB over the Pacific during the months of January and February is considerably less frequent than in other months. Wintertime PWB can, however, be quite dramatic due to exaggerated wave amplitudes, strong wave activity fluxes, and deep vertical extent.

The frequency of PWB over the Pacific increases throughout the spring. This coincides with the weakening and contraction of the jet and the PV barrier (see Fig. 5c). As a result, the surf zone shifts gradually westward and poleward into the central Pacific (Fig. 5d). Between March and April the jet over the central Pacific basin weakens and moves poleward 5°–10°. The increased separation of the Pacific jet exit from the North American jet entrance region, coupled with a weakening of the localized meridional PV gradient, leads to nearly twice as many PWB events in April than in March (Fig. 4). Toward the end of spring, the zero-wind line over the western Pacific moves abruptly poleward (also noted in Fleming et al. 1987). This coincides with the shift of maximum PWB frequency westward into the central and western Pacific basin, and upward to the 350- and 360-K surfaces, associated with the development of the Indian–Asian monsoonal circulation.

By summer, the jet moves well poleward and is only half as strong as it was during winter (Fig. 5e). The zero-wind line moves northward to near 30°N across the western Pacific. Wave propagation is therefore restricted to the extratropics over much of the basin. While the PV gradient, coincident with the Asian jet, remains strong over the continent just north of the Himalayas, it abruptly weakens in the jet exit region over the western Pacific. This preconditions the flow over the western and central Pacific basin to wave breaking (Fig. 5f). Note that even though wave forcing is much weaker in summer than in winter, the weak PV gradient in summer is instrumental in allowing the frequent PWB.

Previous studies (e.g., Postel and Hitchman 1999; Dunkerton 1995) have speculated that the monsoonal circulation plays an important role in PWB. Our observations confirm that the highest frequency of breaking events occurs just downstream (east) of the monsoon region in summer. The thermally forced monsoonal circulation forms a prominent closed upper-level anticyclone that dominates the summertime upper-level flow over the Asian continent. Associated with this circulation is an upward-bulging tropopause that forms a large reservoir of anomalously low PV, clearly visible on upper-level isentropic surfaces (360–370 K) (Dethof et al. 1999). The well-defined Asian jet lies just poleward of the upper-level anticyclone, and acts as a dynamical barrier between the low-PV reservoir over the monsoonal region and the high-PV reservoir in the extratropics (stratospheric air) to the north. However, this barrier disappears just northeast of the Asian monsoon in the jet exit region. Quasi-stationary waves (often accompanied by embedded synoptic disturbances) become vulnerable to breaking as they transition between propagating zonally along the strong PV gradient associated with the Asian jet and propagating southeastward over the western Pacific where the PV gradient is quite weak and the zero-wind line extends well poleward. We suggest that the anticyclonic monsoonal circulation acts to precondition the upper troposphere to PWB in the following ways: 1) by creating a reservoir of anomalously low PV extending well outside the Tropics; 2) by enhancing the PV gradient on the northward flank of the monsoonal anticyclone, thus providing support for wave propagation upstream of the breaking region; and 3) by weakening the PV gradient over the western Pacific basin. As the upper-tropospheric monsoonal anticyclone becomes established in late May, we observe a dramatic increase in PWB events. Repetitive wave breaking further weakens the PV gradient over the subtropical Pacific basin, leading to the formation of the surf zone. The extent to which the interannual variability of summertime PWB over the western Pacific is characterized by the interannual variability of the monsoon is further discussed in section 4a.

Wave breaking is still quite prevalent in fall despite a marked strengthening of the jet (Fig. 5g). Much in line with the seasonal progression of the flow field, the preferred location for PWB migrates eastward and equatorward across the ocean basin (Fig. 5h). The seasonal asymmetry in the frequency of PWB between spring and fall is remarkable, with significantly more events in fall, which is in agreement with Haynes and Shuck-

burgh (2000). Although the westerly jet is slightly stronger in fall, it is displaced well poleward from its location in spring (Fig. 5g). Similarly, the zero-wind line is located near 20°N in fall, compared to 10°N in spring. Finally, we observe that the equatorward-directed wave activity flux is stronger in fall. This may in part be attributed to the close correspondence between the latitude of the jet and that of orographic forcing (Fleming et al. 1987). The net result of the aforementioned dynamical features leads to increased frequency of PWB in fall compared to spring.

b. Atlantic

Winter is the only season when PWB is observed to occur more frequently over the Atlantic basin than over the Pacific basin. The eddy-driven and subtropical jets over the Pacific are nearly collocated during winter, thus contributing to a stronger jet that is more resistant to PWB. However, the Atlantic in winter is characterized by a significant meridional separation between the eddy-driven and subtropical jets (Thompson et al. 2002). The weaker flow (and corresponding weaker PV gradient) over the subtropical Atlantic makes the area more prone to PWB than the Pacific. Additionally, significant interannual variability in PWB frequency is observed over the subtropical North Atlantic in winter. As will be discussed in section 4c, changes in the time-mean flow associated with the phase of the NAO result in changes in wave activity flux, which consequently influence the frequency of PWB.

Unlike the increase in PWB in spring over the Pacific, over the Atlantic PWB decreases in spring (Fig. 5d). The upper-level subtropical PV gradient strengthens in March, leading to the formation of an uninterrupted band of a rather strong PV gradient stretching across the Atlantic basin into North Africa (not shown). The enhanced PV gradient closes the horizontal gap between the North Atlantic jet exit and the North African–Asian jet entrance, creating a near-continuous waveguide over the subtropical Atlantic. This inhibits equatorward wave propagation, thus decreasing the frequency of PWB in spring.

A dramatic increase in PWB events takes place in June as the surf zone over the western half of the subtropical Atlantic basin becomes quite active (Fig. 4). The onset of active PWB coincides with an abrupt weakening of the climatological jet and a poleward displacement of the zero-wind line (not shown, Fig. 5e shows the JJA mean). PWB events are observed over a region from the southeastern seaboard of the United States and the Caribbean to over the central subtropical Atlantic (Fig. 5f).

The North American monsoon may play a similar role to that of the Asian monsoon in preconditioning the flow to PWB over the Atlantic basin. The pronounced increase in PWB frequency on the 350-K surface in summer (Fig. 4c) and decrease on lower isentropic surfaces suggest that the North American monsoon pushes the tropopause to higher vertical levels. However, PWB frequency on the 360-K surface is negligible over the Atlantic compared to that over the Pacific. This may be due to fact that the North American monsoon is weaker and does not penetrate as deeply as the Indian–Asian monsoon (Dunkerton 1995). The delayed onset of the North American monsoon compared to the Asian monsoon may help explain the observed 1-month delay in the onset of active PWB in the Atlantic compared to that in the Pacific.

During the months of September and October, PWB remains quite active over the subtropical Atlantic. Seasonal asymmetry in PWB between the spring and fall seasons is even more striking in the Atlantic basin than in the Pacific basin because breaking is nearly as frequent in fall as it is during summer (Fig. 4). The upper-tropospheric latitudinal PV gradient (and the closely related zonal wind field) is quite different in fall from that in spring. In fall the jet and the zero-wind line are displaced about 10° poleward of their springtime location. This results in a gap in the North Atlantic waveguide in fall and increased wave breaking.

4. Interannual variability

a. East Asian summer monsoon

The Indian–Asian summer monsoon is a massive and complex feature that dominates the large-scale NH flow fields in summer. Although there have been many different attempts to quantify the strength of the monsoon (i.e., monsoon indices), very few use the upper-tropospheric signature of the monsoonal circulation. The extension of the monsoonal anticyclone toward the northeast appears instrumental in increasing PWB frequency. The East Asian summer monsoon (EASM) index, or regional monsoon index RM2I (Lau et al. 2000), serves as a suitable index for documenting the interannual variability of PWB as it relates to the monsoon circulation (and the subtropical jet) over the eastern Asian–western Pacific region. This index is defined as follows:

$$\mathrm{RM2} = \overline{<u_{200}[40 - 50°\mathrm{N}, 110 - 150°\mathrm{E}]>} - \overline{<u_{200}[25 - 35°\mathrm{N}, 110 - 150°\mathrm{E}]>},$$

$$\mathrm{RM2I} = \mathrm{RM2} - \widehat{\mathrm{RM2}},$$

where u_{200} is the zonal wind at 200 hPa, the brackets indicate an area average, the overbar is the seasonal

mean over JJA, and the hat indicates the climatological JJA mean. A strong EASM (i.e., positive values of RM2I) features a strong upper-tropospheric anticyclone over East Asia (distinctly separated from the dominant anticyclone over Pakistan) as well as a northward shift of the subtropical jet. Composites of anomalous EASM indices are formed from those exceeding one standard deviation (σ) from the mean.

Interannual variability in surf zone activity over the west Pacific, inherently linked to the strength and extent of the Asian jet, appears to be associated with interannual variability in the EASM. This is verified by noting a significant correlation $r = 0.412$ (>99% significance) between the summer mean RM2I and the number of wave-breaking events west of the date line. This relation is particularly strong in early summer (June–July), but is likely less important in late summer, especially compared to other features of the East Asian circulation, such as the Bonin high (Enomoto et al. 2003).

Over the west Pacific (130°E–180°), we find a 60% increase in PWB frequency during the positive phase of the EASM (RM2I $\geq \sigma$) compared to the negative phase (RM2I $\leq -\sigma$). During the positive phase of the EASM, the jet shifts northwestward and the zero-wind line moves 5° poleward over the west Pacific (Fig. 6a). In addition, the PV barrier retreats westward over the Asian continent allowing for a significant weakening in the latitudinal PV gradient near the east coast of Japan. This modulation in the Asian jet weakens the waveguide over the west Pacific and favors PWB. During the positive phase of the EASM, we observe an extensive region where the PV gradient is negative across much of the Pacific (not shown). This signature is indicative of an active surf zone.

During the negative phase of the EASM, the jet extends farther east off the coast of Asia and shifts equatorward, resulting in a stronger latitudinal PV gradient over the west Pacific (Fig. 6b). This flow field is more likely to support quasi-stationary wave propagation, thus contributing to the observed decline in PWB over the west Pacific. It is interesting to note that during years of weak EASM the frequency of PWB increases in the eastern Pacific, corresponding to a longitudinal shift in the wave-breaking region.

b. ENSO

ENSO is the largest mode of climate variability on interannual time scales with global impacts. Here we examine the effects of ENSO on PWB over the Pacific basin. Significant differences are observed during the mature phase of ENSO, as documented by the winter mean (DJF) Southern Oscillation index (SOI) (Trenberth 1984). Cold (La Niña, SOI $\geq \sigma$) and warm (El Niño, SOI $\leq -\sigma$) ENSO events are defined as winters where the SOI exceeds one standard deviation from the mean.

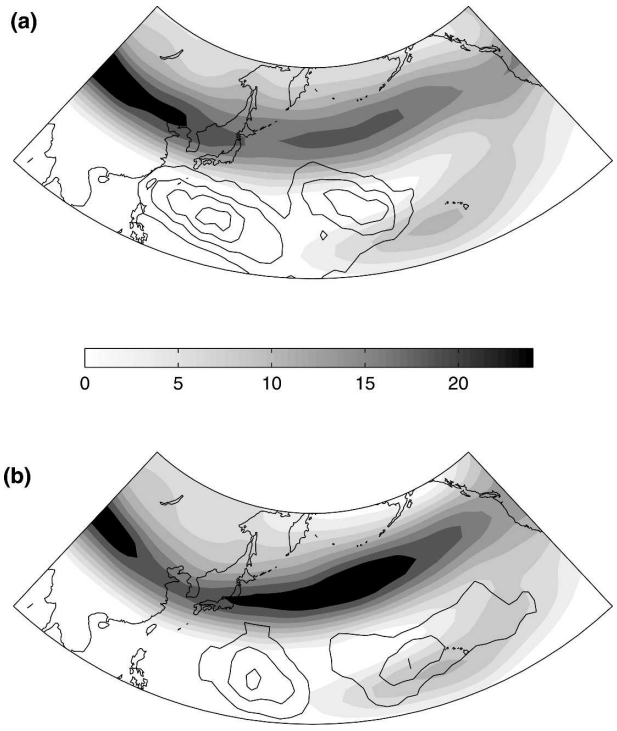

FIG. 6. Composite JJA 250-hPa zonal wind for (a) EASM positive and (b) EASM negative. Contours show PWB number density per season. Contour interval is one per season (starting at two per season).

A strong correlation $r = 0.565$ (>99% significance) exists between the number of PWB during winter over the eastern Pacific and the SOI. We find that the frequency of PWB during La Niña winters is more than double that during ENSO-neutral winters, and the frequency of PWB is drastically reduced during El Niño winters compared to ENSO-neutral winters. These results are consistent with the interannual variability of PV intrusion events, when tongues of high PV reach the deep Tropics even though PWB may not take place (Waugh and Polvani 2000). During La Niña the eastern Pacific zonal flow is weaker (Fig. 7a), resulting in increased PWB in the subtropical eastern Pacific.

During El Niño winters the subtropical jet extends eastward across the Pacific. An unbroken band of a rather strong latitudinal PV gradient associated with the strengthened subtropical jet forms a near-continuous waveguide over the Pacific basin (Fig. 7b). The flow field during El Niño winters is more apt to support wave propagation, thereby inhibiting equatorward penetration of wave activity into the Tropics and decreasing the likelihood of PWB.

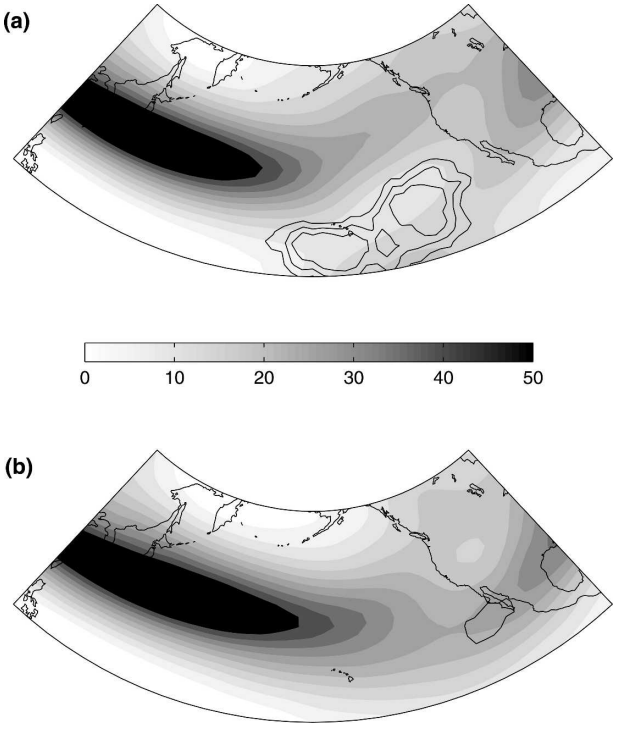

FIG. 7. Composite DJF 250-hPa zonal winds for (a) La Niña and (b) El Niño. Contours show PWB number density per season. Contour interval is 0.5 per season (starting at 1 per season).

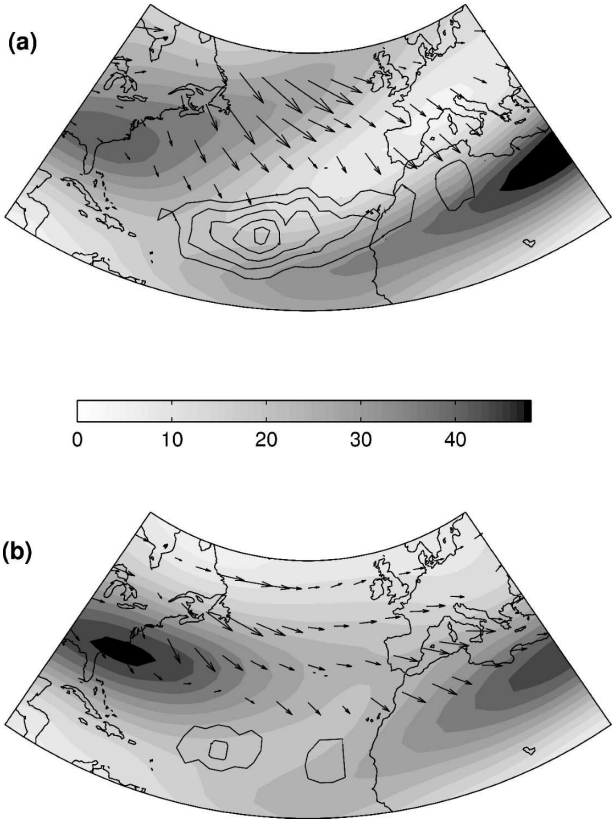

FIG. 8. Composite DJF 300-hPa zonal winds for (a) NAO positive and (b) NAO negative. Stationary wave activity flux at 300 hPa is superposed. The largest vector shown is of magnitude 35 $m^2 s^{-2}$. Contours show PWB number density per season. Contour interval is 0.5 per season (starting at 1 per season).

c. NAO

The NAO appears as the dominant mode of low-frequency variability during the winter season over the North Atlantic sector. PWB over the Atlantic in winter has a strong interannual signal that is closely tied to the phase of the NAO, which is quantified by the first rotated empirical orthogonal function of the 500-hPa geopotential height field over the NH poleward of 20°N. NAO-positive (negative) winters are defined as those winters having an NAO index exceeding one standard deviation from the mean in the positive (negative) direction. We find a correlation of $r = 0.505$ (>99% significance) between the total number of PWB events each winter and the winter mean NAO index. Furthermore, more than twice as many PWB events are observed during NAO-positive winters than NAO negative winters.

Composites of upper-tropospheric zonal wind for both signs of the NAO are shown in Fig. 8. During the positive NAO, the eddy-driven part of the jet acquires a pronounced northward tilt and shifts farther poleward from the subtropical part of the jet (Fig. 8a). As a result, the flow field across the subtropical Atlantic is weaker, leading to conditions favorable to PWB. During the negative NAO, the jet shifts equatorward and assumes a more zonally oriented path across the North Atlantic (Fig. 8b). The zonally oriented jet forms a near-continuous waveguide across the Atlantic that gives enhanced support for quasi-stationary wave propagation and limits PWB over the basin.

The composite flow fields associated with the two signs of NAO show different signals in the stationary wave activity flux. For NAO-positive winters, the equatorward-directed wave activity flux over the North Atlantic is enhanced (Fig. 8a) resulting from increased equatorward wave propagation (e.g., Limpasuvan and Hartmann 1999). The enhanced equatorward wave–activity flux combined with weaker westerly flow over the central and eastern Atlantic near 30°N result in more frequent PWB. Conversely, during NAO-negative winters, the equatorward wave activity flux over the North Atlantic is significantly reduced (Fig. 8b). At the same time the westerly flow is stronger near 30°N, favoring zonal Rossby wave propagation and decreasing the likelihood of PWB.

The strong poleward eddy momentum flux associ-

ated with wintertime PWB over the Atlantic may, in turn, influence the NAO. On intraseasonal time scales our observational analysis suggests that PWB over the Atlantic is concurrent with the positive phase of the NAO (Abatzoglou and Magnusdottir 2006). The manner in which PWB on synoptic and intraseasonal time scales relates to the identified interannual relationship is not fully established at this time.

5. Nonlinear reflection

Nonlinear reflection is observed in 36% of PWB events. A PWB event is classified as reflective when a poleward-directed wave activity flux is observed downstream and poleward of the wave-breaking region following wave breaking as described in section 2b. Daily composite lead–lag maps of 250-hPa eddy meridional wind corroborate that nonlinear reflection is taking place. Figure 9 shows composite maps for reflective PWB cases, depicting eddy meridional wind (contours) and the latitudinal PV gradient (shaded). Prior to breaking, a wave train with positively (northeast–southwest) tilted phase lines is seen propagating eastward and equatorward. As PWB takes place, the PV field (not shown) becomes irreversibly deformed leading to the abrupt termination of linear wave propagation. Following the breaking the wave train appears to split. A portion of the wave train is seen proceeding into the subtropics equatorward of the breaking point, where it disappears within a few days. This is indicative of wave absorption. A secondary wave train can be seen emerging from the wave-breaking region 2–3 days after the break. This poleward-arching wave train with negatively (northwest–southeast) tilted phase lines propagates downstream from the wave-breaking region (Figs. 9d–e). The signature seen here in observations is quite similar to that seen in a hierarchy of modeling experiments (Walker and Magnusdottir 2003, and references therein). Linear wave propagation is not possible within the wave-breaking region where the PV field is mixed. The reflected wave train appears off the northeast edge of the wave-breaking region where the latitudinal PV gradient remains strong enough to support linear wave propagation.

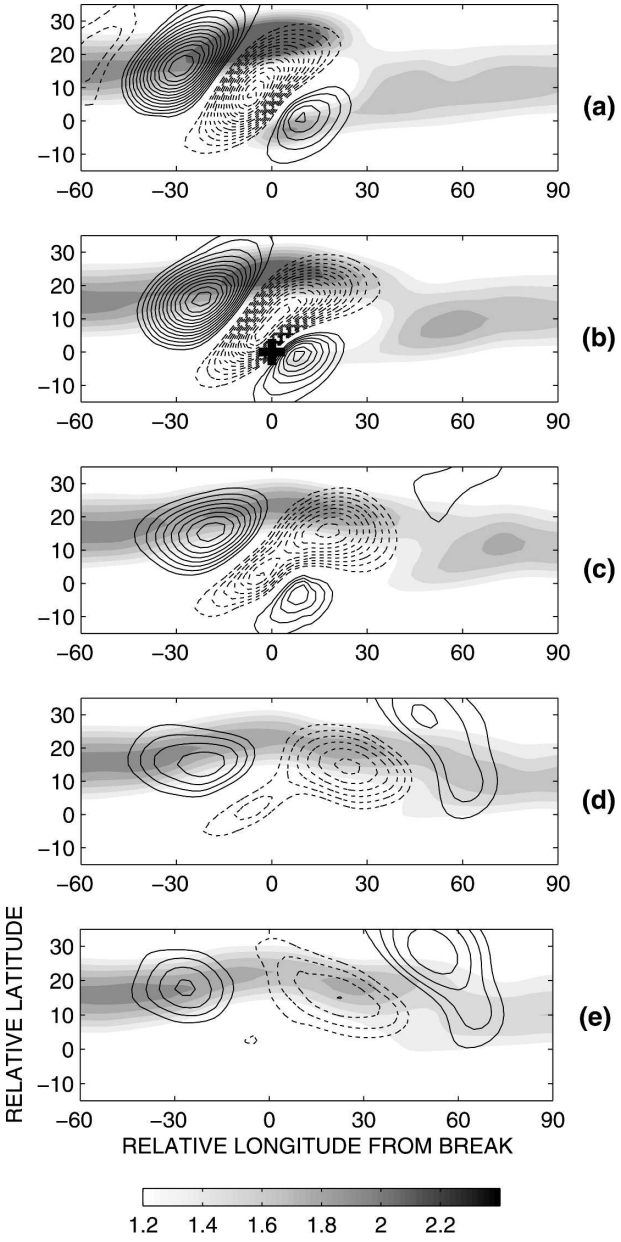

FIG. 9. Composite 250-hPa eddy meridional wind for reflective PWB. Daily composites are shown, from (a)–(e) 1 day before to 3 days following the day when breaking (+) is first noted. The contour interval is 1 m s^{-1} for values greater than 2 m s^{-1}. Solid (dashed) contours represent poleward (equatorward) flow. Shading indicates the composite daily latitudinal PV gradient on 350 K in units of 1×10^{-6} PVU m^{-1}.

The same composite daily fields for PWB cases with no return flux of wave activity show a different signature following wave breaking (Fig. 10). Similar to the reflective composite, the wave train splits following PWB with one branch being absorbed within the wave-breaking region. Unlike the reflective composite, the poleward branch shows continued equatorward propagation, eventually disappearing in the subtropics downstream of the breaking point a few days later. The latitudinal PV gradient in this composite is the weakest in the area where the reflected wave train emerged in Fig. 9, northeast of the wave-breaking region. Daily PV fields show that many of these nonreflective events do not break rapidly (within 1 day). Instead, they meet the wave-breaking criteria in the days following initial di-

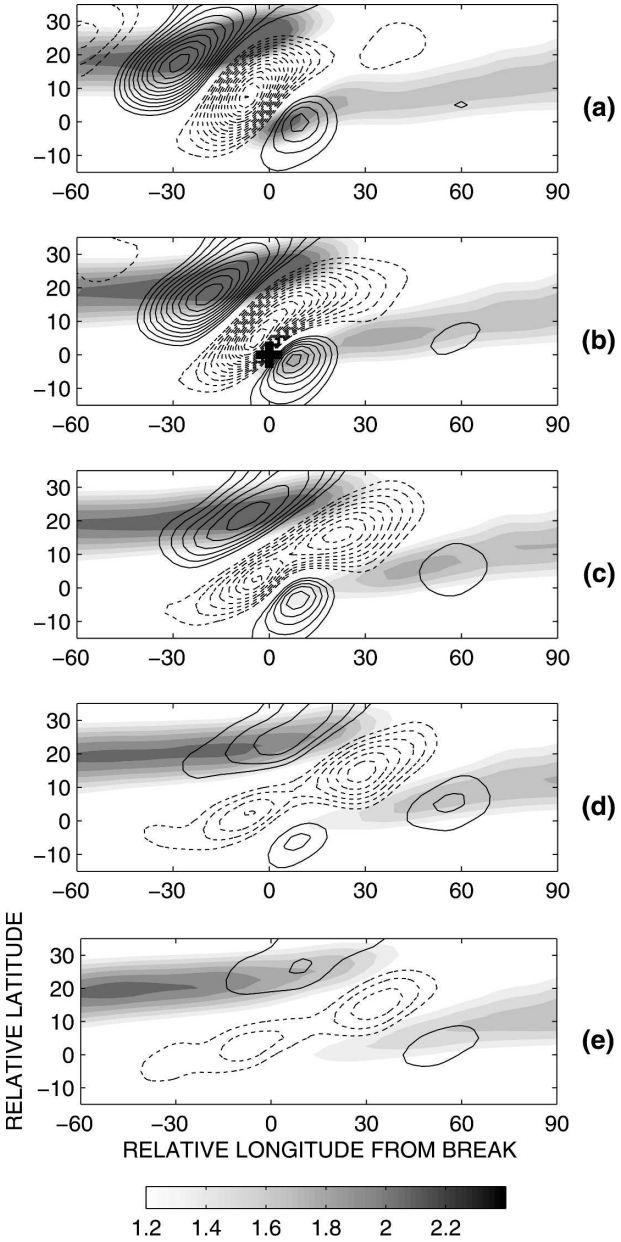

FIG. 10. Same as Fig. 9, but for nonreflective PWB.

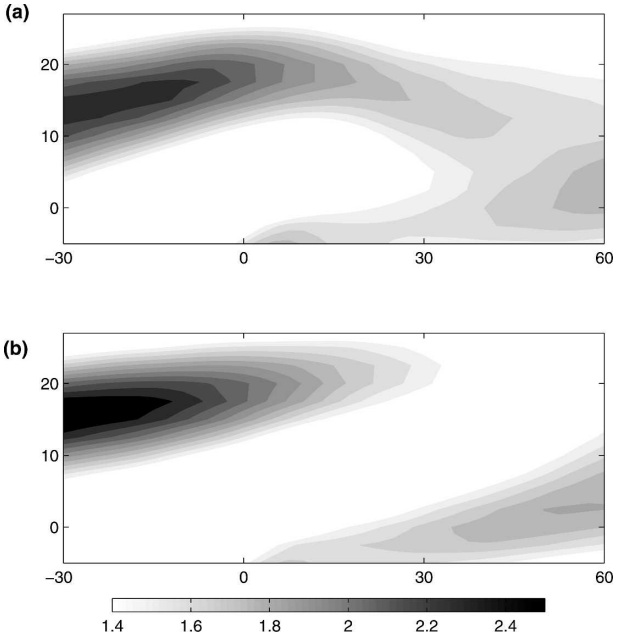

FIG. 11. Composite of the 21-day time-mean latitudinal PV gradient on the 350-K isentropic surface for (a) reflective and (b) nonreflective PWB. Units are 1.0×10^{-6} PVU m^{-1}.

agnosis. Prolonged breaking allows dissipation to act over an extended time period leading to absorption of wave activity.

According to our daily composite analysis, the PV gradient in the area where the reflected wave train emerges out of the wave-breaking region must be above a critical value for nonlinear reflection to proceed. In Fig. 11 we examine the 21-day time mean of the latitudinal PV gradient for the composite of reflective (Fig. 11a) and nonreflective (Fig. 11b) PWB events. A comparison of the two peaks reveals that the latitudinal PV gradient is substantially weaker over a broad region for the nonreflective case (Fig. 11b).

In section 3 we found that the annual cycle of zonal flow in many ways dictates the strength and location of the wave-breaking region. One may wonder whether seasonal changes in zonal flow downstream of the wave-breaking region can alter the probability of nonlinear reflection. Unlike the very striking seasonality in PWB, the proportion of PWB events that results in reflection only depends weakly on season. Over both ocean basins nonlinear reflection tends to be favored during the transition seasons of spring and fall, and is least likely to occur during winter (Fig. 12a). The rather unvarying ratio of reflective events as a function of season suggests that in order to determine the upshot of PWB one must consider PV gradient for each event rather than simply the climatological flow.

Over 45% of PWB events occurring in spring and fall are identified as reflective. A rather strong PV gradient, associated with the east Pacific subtropical jet and North African–Asian jet, exists downstream of the respective surf zones over the Pacific and Atlantic during the transition seasons. We believe that the juxtaposition of these surf zones to the downstream jet entrance regions largely accounts for the increase in the ratio of nonlinear reflection. Consistent with the above argument, Fig. 12b details that reflection is favored over the eastern ocean basins just upstream of the North American and North African jet entrance regions. Remark-

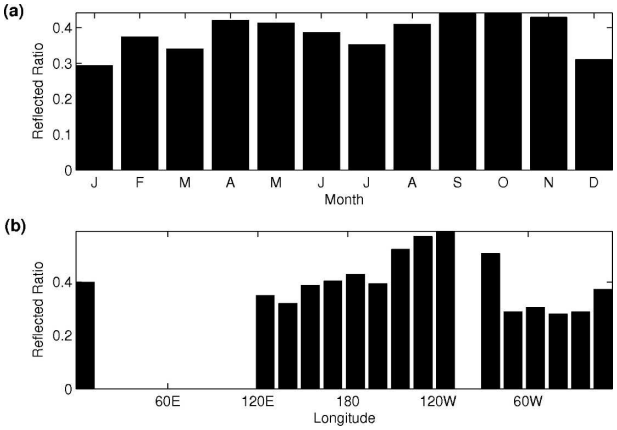

FIG. 12. Ratio of PWB events that result in nonlinear reflection by (a) month and (b) longitude. Longitudinal sectors with fewer than 15 total PWB events over the 46-yr period are omitted.

ably, nonlinear reflection is found in nearly 60% of all PWB events occurring over the eastern Pacific and west coast of North America.

In winter, despite increased wave forcing and a stronger PV gradient, less than 30% of PWB are found to be reflective. This decrease in nonlinear reflection may be due to the strong wintertime Hadley circulation. The Hadley circulation has been shown to act as an absorber of wave activity and inhibitor of nonlinear reflection (Magnusdottir and Walker 2000; Walker and Magnusdottir 2002). We believe that the possibility of nonlinear reflection goes down as the subtropical upper troposphere is better able to absorb the equatorward wave activity flux.

While we have shown that the PV gradient is an important factor in determining whether nonlinear reflection can take place, this result does not hold true for all cases. We have identified nonreflective (reflective) cases with a strong (weak) PV gradient downstream of the breaking region. Nonetheless, by selecting PWB events where the PV gradient is enhanced (i.e., greater than the average) in the region of interest, nonreflective events are selectively filtered out.

Observations have shown that equatorward penetration of planetary waves can lead to deep convection in the Tropics, especially in winter (Kiladis 1998). Thus, one might speculate that the secondary or reflected wave train directed into the extratropics results from deep convection. However, we found no evidence of enhanced convection (as indicated by low outgoing longwave radiation) associated with the reflective PWB events. Upon finding no such signal, we concluded that the secondary wave train was indeed the result of nonlinear reflection.

6. Concluding remarks

We have objectively identified anticyclonic Rossby wave–breaking events on isentropic surfaces near the subtropical tropopause in 46 yr of daily averaged National Centers for Environmental Prediction–National Center for Atmospheric Research (NCEP–NCAR) reanalysis data. The large-scale breaking events that we analyze are almost exclusively associated with quasi-stationary planetary waves with average phase speeds around 2 m s^{-1}. The majority of these PWB events occur during JJA over the subtropical ocean basins in the NH. Nonetheless, a well-defined surf zone is observed in every season near the jet exit region over the two NH ocean basins, where the upper-tropospheric zonal wind and the latitudinal PV gradient are weak. Seasonal evolution of the jet largely accounts for seasonal changes in the location and frequency of PWB. As the jet expands and contracts, the surf zone moves eastward and equatorward in fall, returning westward and poleward in spring. Over both ocean basins, the frequency of PWB increases rather dramatically in late spring, coinciding with the rapid weakening of the subtropical jet and the poleward movement of the zero-wind line.

Significant interannual variability in PWB over both the Pacific and the Atlantic is shown to pertain to several well-known modes of climate variability. During positive EASM summers the weaker Rossby waveguide over the Pacific leads to increased PWB. In winter, the dominant climate modes over both the Pacific and Atlantic strongly influence the frequency of PWB. Over the eastern Pacific, PWB is substantially reduced during El Niño winters and increased during La Niña winters. Over the North Atlantic, a strong correlation is found between wintertime PWB and the positive NAO. The poleward shift in the eddy-driven jet and the enhanced equatorward wave activity flux during a positive NAO winter primes the central and eastern subtropical Atlantic for wave breaking.

Nearly 36% of all PWB events result in nonlinear reflection. For these cases we observe a poleward-arching wave train with northwest–southeast-oriented phase lines emanating from the wave-breaking region in the days following PWB. Conversely, for nonreflective (absorptive) events, the wave train appears to stagnate and eventually decay in the subtropics. For nonreflective cases the PV field indicates that breaking is prolonged, lasting several days after breaking is initially diagnosed (not shown). These nonreflective prolonged breaking events deposit wave activity over a zonally broadened region in the subtropics.

Our analysis reveals that the latitudinal PV gradient immediately northeast of the wave-breaking region is

stronger when nonlinear reflection takes place following PWB than when it does not take place. This may provide a constraint in determining whether nonlinear reflection is possible. A reflected wave train can escape the wave-breaking region if the PV gradient downstream of the wave-breaking region will allow linear wave propagation. In the presence of a weak PV gradient, the support for linear wave propagation (i.e., the reflected wave train) is simply not there. Previous studies have focused on wave forcing (and the resulting wave amplitude) as the most important factor in determining the possibility of nonlinear reflection. To examine the role of wave forcing on the reflective/absorptive behavior of PWB, we relaxed the first criterion of our algorithm to detect PWB (section 2a), such that PWB is diagnosed when a region of 2 PVU (instead of 3 PVU) is equatorward of a region of 1 PVU. While this nearly doubles the total number of PWB events, the proportion of reflective events only decreases slightly (from 36% to 31%). This suggests that although wave amplitude is an important parameter in determining the possibility of nonlinear reflection, other features related to the flow downstream are equally important.

Acknowledgments. We thank Sukyoung Lee and two other reviewers for comments and suggestions that improved the manuscript. This work was supported by NSF Grant 0301800 and NOAA grant NA06OAR4310149. We thank NCAR's SCD for providing the reanalysis datasets.

REFERENCES

Abatzoglou, J. T., and G. Magnusdottir, 2004: Nonlinear planetary wave reflection in the troposphere. *Geophys. Res. Lett.,* **31,** L09101, doi:10.1029/2004GL019495.

——, and ——, 2006: Opposing effects of reflective and nonreflective planetary wave breaking on the NAO. *J. Atmos. Sci.,* in press.

Brunet, G., and P. H. Haynes, 1996: Low-latitude reflection of Rossby wave trains. *J. Atmos. Sci.,* **53,** 482–496.

Dethof, A., A. O'Neill, J. M. Slingo, and H. G. J. Smit, 1999: A mechanism for moistening the lower stratosphere involving the Asian summer monsoon. *Quart. J. Roy. Meteor. Soc.,* **125,** 1079–1106.

Dunkerton, T. J., 1995: Evidence of meridional motion in the summer lower stratosphere adjacent to monsoon regions. *J. Geophys. Res.,* **100,** 16 675–16 688.

Enomoto, T., B. J. Hoskins, and Y. Matsuda, 2003: The formation mechanism of the Bonin high in August. *Quart. J. Roy. Meteor. Soc.,* **129,** 157–178.

Fleming, E. L., G. H. Lim, and J. M. Wallace, 1987: Differences between the spring and autumn circulation of the Northern Hemisphere. *J. Atmos. Sci.,* **44,** 1266–1286.

Haynes, P. H., and E. F. Shuckburgh, 2000: Effective diffusivity as a diagnostic of atmospheric transport. Part II: Troposphere and lower stratosphere. *J. Geophys. Res.,* **105,** 22 795–22 810.

Held, I. M., M. Ting, and H. Wang, 2002: Northern winter stationary waves: Theory and modeling. *J. Climate,* **15,** 2125–2144.

Hoinka, K. P., 1999: Temperature, humidity, and wind at the global tropopause. *Mon. Wea. Rev.,* **127,** 2248–2265.

Holton, J. R., P. H. Haynes, M. E. McIntyre, A. R. Douglass, R. B. Rood, and L. Pfister, 1995: Stratoshere-troposphere exchange. *Rev. Geophys.,* **33,** 403–439.

Hsu, C. J., M. J. Prather, and O. Wild, 2005: Diagnosing the stratosphere-to-troposphere flux of ozone in a chemistry transport model. *J. Geophys. Res.,* **110,** D19305, doi:10.1029/2005JD006045.

Kiladis, G. N., 1998: Observations of Rossby saves linked to convection over the eastern tropical Pacific. *J. Atmos. Sci.,* **55,** 321–339.

Lau, K. M., K. M. Kim, and S. Yang, 2000: Dynamical and boundary forcing characteristics of regional components of the Asian summer monsoon. *J. Climate,* **13,** 2461–2482.

Limpasuvan, V., and D. Hartmann, 1999: Eddies and the annular modes of climate variability. *Geophys. Res. Lett.,* **26,** 3133–3136.

Magnusdottir, G., and P. H. Haynes, 1999: Reflection of planetary waves in three-dimensional tropospheric flows. *J. Atmos. Sci.,* **56,** 652–670.

——, and C. C. Walker, 2000: On the effects of the Hadley circulation and westerly equatorial flow on planetary-wave reflection. *Quart. J. Roy. Meteor. Soc.,* **126,** 2725–2745.

McIntyre, M. E., and T. N. Palmer, 1983: Breaking planetary waves in the stratosphere. *Nature,* **305,** 593–600.

Plumb, A. R., 1985: On the three-dimensional propagation of stationary waves. *J. Atmos. Sci.,* **42,** 217–229.

Postel, G. A., and M. H. Hitchman, 1999: A climatology of Rossby wave breaking along the subtropical tropopause. *J. Atmos. Sci.,* **56,** 359–373.

Thompson, D. W. J., S. Lee, and M. P. Baldwin, 2002: Atmospheric processes governing the Northern Hemisphere annular mode/North Atlantic Oscillation. *North Atlantic Oscillation: Climate Significance and Environmental Impact, Geophys. Monogr.,* Vol. 134, Amer. Geophys. Union, 81–112.

Trenberth, K. E., 1984: Signal versus noise in the Southern Oscillation. *Mon. Wea. Rev.,* **112,** 326–332.

Walker, C. C., and G. Magnusdottir, 2002: Effect of the Hadley circulation on the reflection of planetary waves in three-dimensional tropospheric flows. *J. Atmos. Sci.,* **59,** 2846–2859.

——, and ——, 2003: Nonlinear planetary wave reflection in an atmospheric GCM. *J. Atmos. Sci.,* **60,** 279–286.

Waugh, D. W., and L. M. Polvani, 2000: Climatology of intrusions into the tropical upper troposphere. *Geophys. Res. Lett.,* **27,** 3857–3860.